Supplement of The Cryosphere, 18, 3723–3740, 2024
https://doi.org/10.5194/tc-18-3723-2024-supplement

The Cryosphere Open Access EGU

Supplement of

Toward long-term monitoring of regional permafrost thaw with satellite interferometric synthetic aperture radar

Taha Sadeghi Chorsi et al.

Correspondence to: Taha Sadeghi Chorsi (taha4@usf.edu)

S1. Introduction

The material in this supplement includes information on the radar interferograms used in this study (Table S1), and a comparison of radar phase coherence at our two study sites, the area around CALM site U8 in northern Alaska's continuous permafrost zone, and the Beta experiment area around CALM site U18 in central Alaska's discontinuous permafrost zone (Figure S1). We also compare the radar-based estimates of ALT and ground-truth data at CALM site U8 (Figure S2).

We then discuss ICESat-2 uncertainties, including a comparison of the ATL06 ('land ice height') and ATL08 ('terrain and vegetation height') data products (Tables S2, S3 and Figures S3, S4, and S5).

Table S1. Sentinel-1 interferograms used in this study. Scene path and frame numbers are 131 and 357, respectively. Satellite direction is descending. Dates are in YYYYMMDD format.

Interferogram [Date1_Date2]	Average Spatial Coherence	Time interval [Days]
20170612_20170624	0.68	12
20170624_20170706	0.54	12
20170706_20170718	0.57	12
20170718_20170730	0.61	12
20170730_20170811	0.81	12
20170730_20170823	0.68	24
20170811_20170823	0.85	12
20170811_20170904	0.64	24
20170823_20170904	0.76	12
20180607_20180619	0.49	12
20180619_20180701	0.63	12
20180701_20180713	0.71	12
20180725_20180806	0.75	12
20180725_20180818	0.66	24
20180725_20180830	0.66	36
20180806_20180830	0.73	24

20180806_20180911	0.67	36
20180818_20180830	0.85	12
20180818_20180911	0.67	24
20180830_20180911	0.8	12
20190602_20190614	0.71	12
20190602_20190626	0.51	24
20190626_20190708	0.58	12
20190708_20190720	0.6	12
20190708_20190801	0.56	24
20190720_20190801	0.8	12
20190720_20190813	0.67	24
20190801_20190813	0.76	12
20190801_20190825	0.51	24
20190813_20190825	0.82	12
20190825_20190906	0.6	12
20200608_20200620	0.7	12
20200620_20200714	0.47	24
20200714_20200726	0.85	12
20200714_20200807	0.48	24
20200726_20200807	0.73	12
20200807_20200819	0.79	12
20200726_20200819	0.54	24
20210603_20210615	0.48	12
20210615_20210627	0.72	12
20210627_20210709	0.57	12
20210709_20210721	0.57	12

20210709_20210802	0.59	24
20210709_20210814	0.54	36
20210709_20210826	0.52	48
20210721_20210802	0.53	12
20210721_20210814	0.75	24
20210721_20210826	0.55	36
20210721_20210907	0.5	48
20210802_20210814	0.71	12
20210802_20210826	0.8	24
20210802_20210907	0.6	36
20210814_20210826	0.89	12
20210814_20210907	0.83	24
20210826_20210907	0.85	12
20220610_20220622	0.6	12
20220622_20220704	0.58	12
20220622_20220716	0.43	24
20220704_20220716	0.69	12
20220716_20220728	0.51	12
20220716_20220809	0.59	24
20220716_20220821	0.52	36
20220728_20220809	0.71	12
20220809_20220821	0.82	12
20220821_20220902	0.71	12

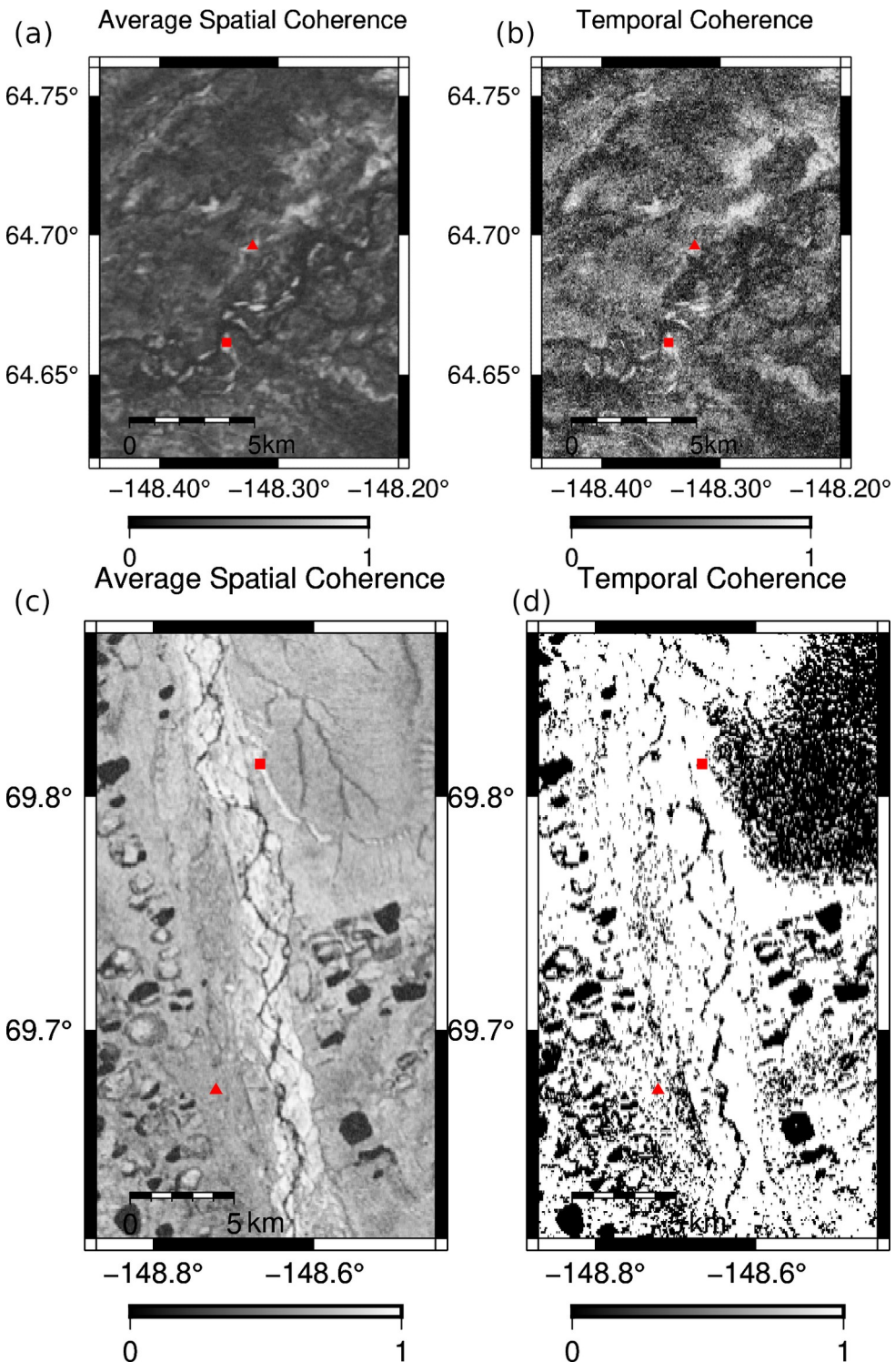

Figure S1. Temporal average of spatial (5 x 5 pixels) coherence (a,c) and temporal (b,d) coherence for the radar data used in our two study sites. **Top**: Study site in the discontinuous permafrost zone southwest of Fairbanks, including CALM site U18 around the Beta experiment area. Note low coherence values. **Bottom**: Study site in the continuous permafrost zone of the Alaskan North Slope, including CALM site U8, with higher spatial and temporal coherence. Red triangles show CALM

locations, red squares show reference point assumed to have minimal motion, selected on the basis of high coherence and expected stability.

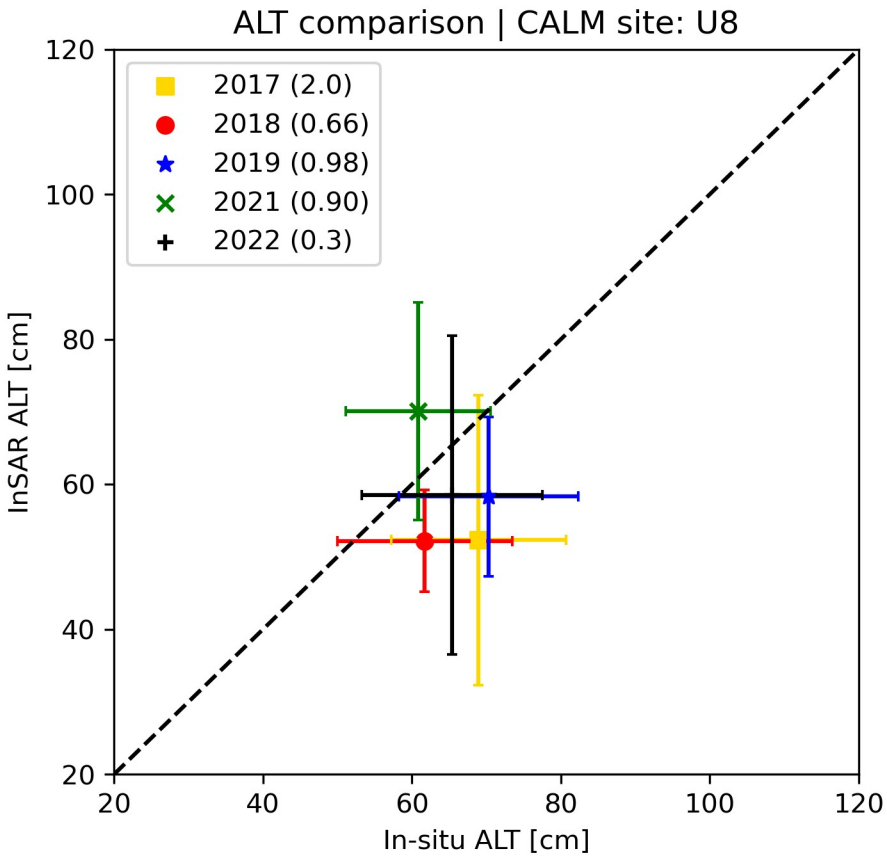

Figure S2. Comparison between in-situ ALT data and ALT estimated from InSAR-measured subsidence combined with a simple physical model. Numbers in parentheses are r^2 (Equation 11).

S2. ICESat-2 Height Products and Uncertainties

The ICESat-2 LiDAR provides elevation and elevation change estimates over most of Earth's surface, mainly limited by cloud cover (Neuenschwander and Pitts, 2019). Depending on application, various height products derived from the satellite raw data are appropriate. The ATL08 height product provides information on both vegetation height and bare earth elevation. The standard deviation of terrain points within the interpolated ground surface for each 100-meter segment along track is reported. The standard deviation for our four test locations ranges from 0.11 m to 0.24 m (Table S2). This parameter is a measure of surface roughness, including vegetation effects. The vegetation type in our study area is

described as graminoid and prostrate-dwarf-shrub vegetation, 5-10 cm in height. Part of the standard deviation reflects different photon returns from bottom, middle and top of vegetation. The impact of this variation on the height estimate is reduced by the ATL08 algorithm, which estimates separate elevations for bare earth and vegetation top.

Neuenschwander et al. (2019) outline various sources contributing to the uncertainty of the ATL08 height product, reflecting both random and systematic errors. These include the precision of the instrument's ranging capabilities, uncertainty in radial orbital positioning, knowledge of geolocation, atmospheric forward scattering, uncertainty in tropospheric path delay, local topography, sampling error, background noise, vegetation, and misidentified photons. The precision of the instrument's ranging primarily depends on the width of the laser pulse and uncertainties in timing electronics. The reported uncertainty is based on error propagation of each of the listed error sources (see equation 1.1 to 1.4 in Neuenschwander et al., 2019). In areas where the surface is relatively flat (slope less than 1 degree) the uncertainty in elevation measurement from in the WGS-84 reference frame is less than 25 cm, taking into account a radial orbital uncertainty of 4 cm and tropospheric path delay uncertainty of 3 cm. This uncertainty grows with steeper slope angles due to factors such as pointing knowledge. Our locations have surface slopes up to ~4 degrees and formal uncertainties as high as 1 m (Table S2). This reflects the accuracy of the 'absolute' height estimate (relative to WGS 84). Relative *changes* of height, the quantity of interest here, can be estimated to higher precision.

Table S2. Reported standard deviation (STD) and uncertainty (UNC) for our four test locations of the ICESat-2 ATL08 product used in this study. Time is in YYYY/MM/DD format.

Location	**Longitude**	**Latitude**	**STD 2021/06/08 [m]**	**STD 2021/09/06 [m]**	**UNC 2021/06/08 [m]**	**UNC 2021/09/06 [m]**
(1)	-148.815	69.826	0.132	0.24	1.018	0.293
(2)	-148.792	69.758	0.129	0.122	0.414	0.93
(3)	-148.787	69.742	0.11	0.125	0.603	0.53
(4)	-148.704	69.755	0.194	0.144	0.675	0.993

Table S3. Reported standard deviation (STD) and uncertainty (sigma_geo_h) for our four test locations of the ICESat-2 ATL06 product used in this study. Time is in YYYY/MM/DD format.

Location	**Longitude**	**Latitude**	**STD 2021/06/08 [m]**	**STD 2021/09/06 [m]**	**sigma_geo_h 2021/06/08 [m]**	**sigma_geo_h 2021/09/06 [m]**
(1)	-148.815	69.826	0.057	0.023	0.215	0.136
(2)	-148.792	69.758	0.032	0.031	0.135	0.127
(3)	-148.787	69.742	0.03	0.027	0.134	0.125
(4)	-148.704	69.755	0.024	0.024	0.135	0.125

The ATL06 algorithm calculates land-ice elevation with high precision at small spatial scales (40 m) while preserving surface slope data along track. This feature aids in distinguishing surface-height measurements from false detection caused by factors like background noise and cloud cover. Across most of the Earth's land ice, the surface typically appears smooth, with minimal variations in slope, less than 1 degree over distances smaller than a few hundred meters (Markus et al., 2017; Smith et al., 2019). The ATL06 height product does not distinguish canopy height and bare earth elevation. Rather, it reports the strongest return for geolocated photons along each 40 m segment, filtered for along-track positioning. It fits a linear model to estimate centroid height and surface slope along each selected segment, and includes instrument bias corrections (Smith et al., 2019).

Smith et al. (2021) lists potential error sources for land-ice products (ATL06) including sampling error, background noise, complex topography, first-photon bias, atmospheric error, misidentified photons and subsurface scattering. Ranging errors and geolocation errors both contribute uncertainty. The reported land-ice height uncertainty (h_li_sigma: STD; Table S3) represents the surface height error resulting *only* from ranging errors. This is determined by propagating error from the least-squares fit of the selected photons and the statistical uncertainty from the first-photon bias correction (Smith et al., 2019). Geolocation errors in both the along-track and cross-track directions are determined using ATL03 parameters and the radial orbit error. These errors are reported in a separate parameter named

“sigma_geo_h” (Smith et al., 2019) listed in table S3 for four selected locations. See also equation 36 in Smith et. (2021).

S3. Previous ICESat-2 Permafrost Studies

Michaelides et al. (2021) conducted a study over Northern Alaska, comparing SBAS-derived deformation with the ATL06 ICESat-2 product (Smith et al., 2019). They used crossover and repeat track data to estimate deformation related to the thaw/freeze cycle. Michaelides et al. (2021) found that large topographic gradients could lead to large differences between ICESat-2 and InSAR-derived estimates, but the two data sets agreed over flatter regions and more uniform landscapes. This suggests that pointing errors have a significant impact on the quality of the LiDAR data.

S4. This Study

The four test locations shown in Figures 1 and 3 have less than 7% slope and show good agreement between InSAR and ICESat-2 LiDAR height change estimates for the 2021 data when the ATL08 product is used. Figure S3 shows the height difference between two epochs and reported standard deviation for ATL08 Section 4.2 provides additional details.

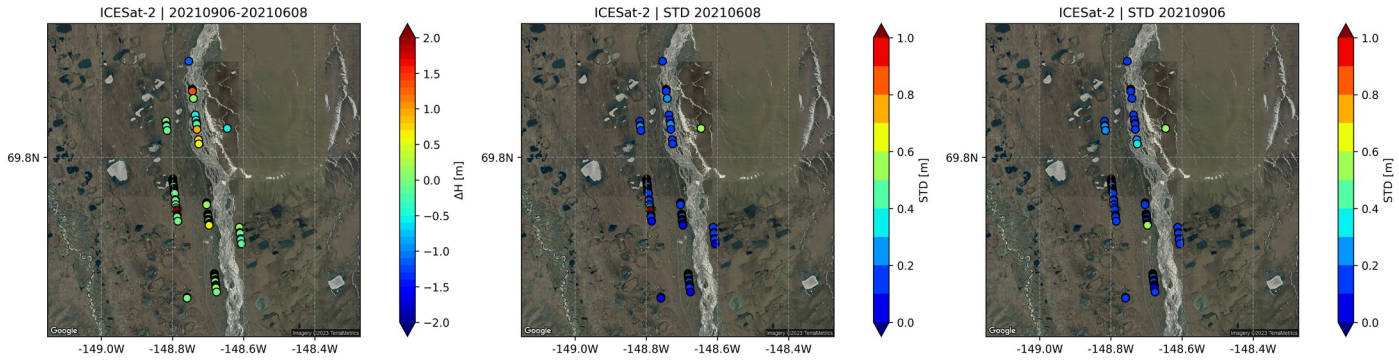

Figure S3. Left panel: ICESat-2 ATL08 best-fitted terrain height (‘h_te_best_fit’) difference between two epochs: 2021-06-08 and 2021-09-06 for study area. Each circle represents height difference between two epochs for 50 m grid cell. See ICESat-2 data processing (4.2) for details. Mid panel: Reported standard deviation of ATL08 product for 2021-06-08 data. Right panel: Reported standard deviation of ATL08 product for 2021-09-06 data. Basemap data is from © 2023 TerraMetrics, Inc./ Google. The maps are produced using Maussion et al., (2021) in Python programming environment.

S5. Comparison of ATL08 and ATL06 Height Products

We compared two higher level height products from ICESat-2 (ATL06 and ATL08) in Northern Alaska along with our InSAR data. As discussed above, ATL06 is optimized to estimate the height of land ice assuming lower slopes and no vegetation, while ATL08 is optimized for more variable terrain with vegetation. While the two height products are similar in our study area, on average ATL08 tends to be a few cm lower in elevation compared to ATL06, presumably reflecting the influence of vegetation and surface roughness in our study area (see Figure S5a). Figures S4 and S5 provide some numerical comparisons between the two height products. Figure S4 shows that two products are generally agree within ~20 cm. ATL06 provides more points mainly due to higher spatial resolution (40 m). 9% of the common area (50 x 50 m resolution cells) agree within 1 cm between the two products. 61% of the common area agree within 10 cm. However, there can be systematic differences between the two height products (Figure S5a). We suggest that ATL08 is a slightly better data product for most permafrost studies, since vegetation is typically present, but may be limited by fewer data points in a given area (Figure S5c).

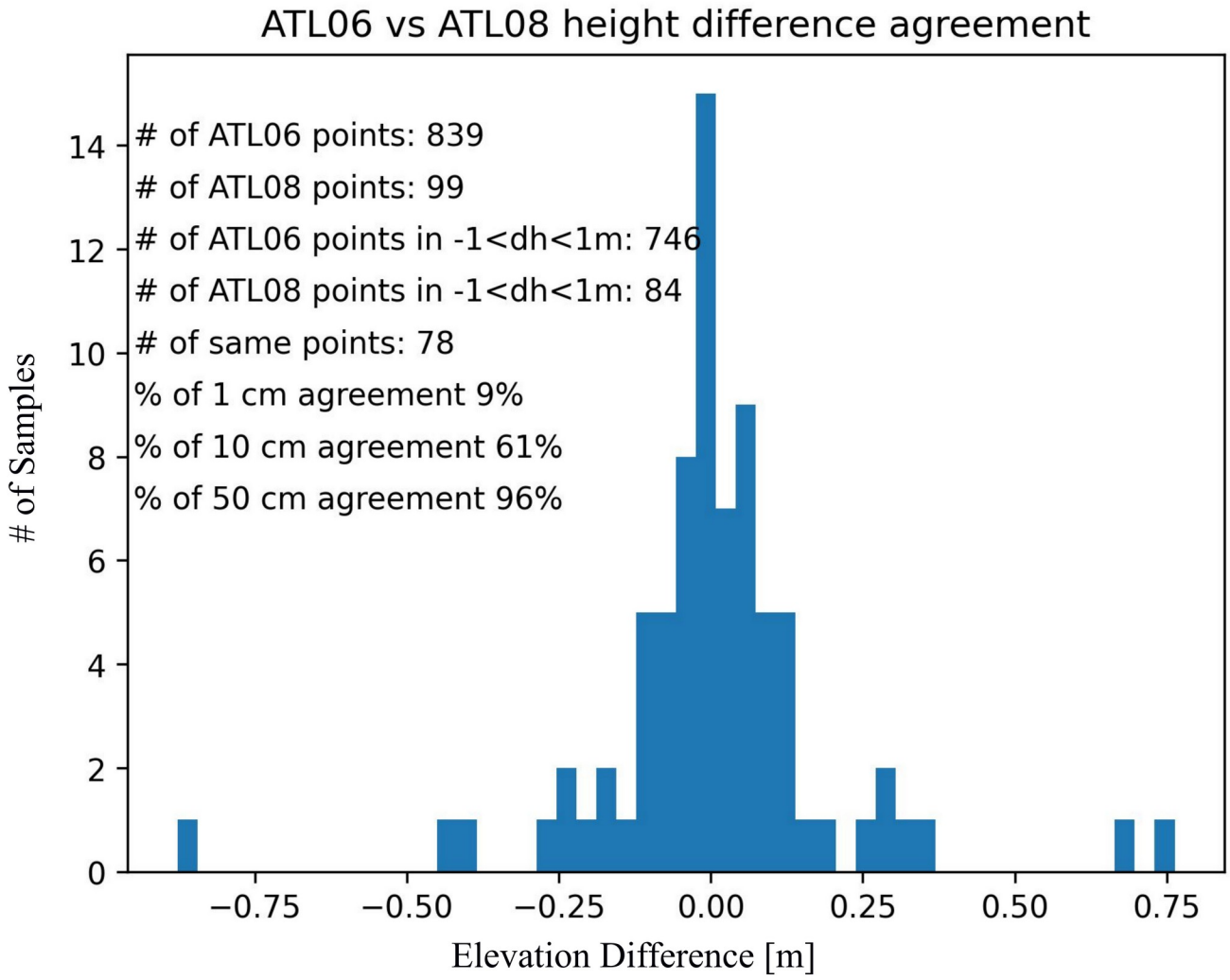

Figure S4. ATL06 and ATL08 height difference agreement for repeat track (reference ground track = 1150) for data 2021-06-08 and 2021-09-06. The two height products generally agree to within 20 cm. The "height difference" calculates by subtracting data in two dates for each product separately.

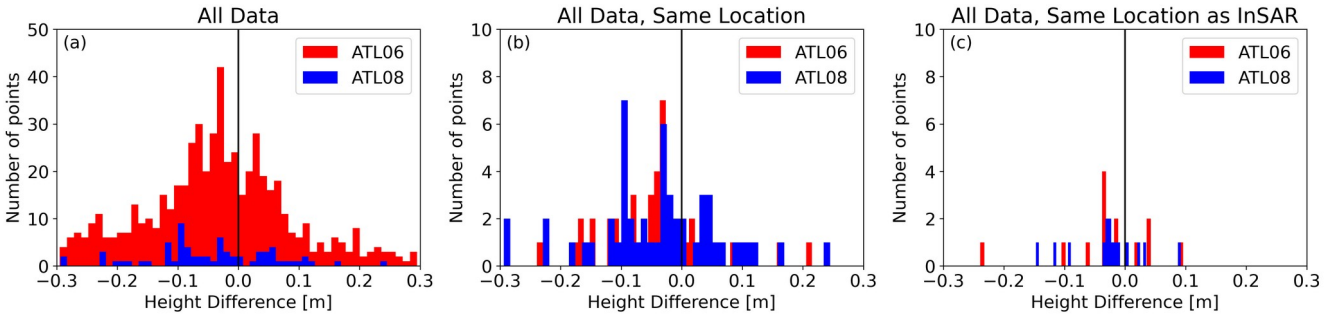

Figure S5. Comparison between ATL06 “h_li” difference and ATL08 “h_te_best_fit” difference of ICESat-2 for (a) all available data in the study area, (b) all available data with same location for both products (read section 4.2 for more detail), and (c) all available data with same location for both ICESat-2 data products and InSAR. X-axis in all panels show height difference between 2021-06-08 and 2021-09-06. Y-axis represents the number of available points. Black vertical line shows zero height difference. The height difference range of different products is cut to ±0.3 m.

S6. References

Markus, T., Neumann, T., Martino, A., Abdalati, W., Brunt, K., Csatho, B., Farrell, S., Fricker, H., Gardner, A., Harding, D., et al.: The Ice, Cloud, and land Elevation Satellite-2 (ICESat-2): science requirements, concept, and implementation, Remote sensing of environment, 190, 260–273, 2017.

Maussion, F., TimoRoth, Landmann, J., Dusch, M., Bell, R., and tbridel: fmaussion/salem: v0.3.4, https://doi.org/10.5281/zenodo.4635291, 2021.

Michaelides, R., Bryant, M., Siegfried, M., and Borsa, A.: Quantifying Surface-Height Change Over a Periglacial Environment With ICESat-2 Laser Altimetry, Earth and Space Science, 8, e2020EA001 538, 2021.

Neuenschwander, A. and Pitts, K.: The ATL08 land and vegetation product for the ICESat-2 Mission, Remote sensing of environment, 221, 247–259, 2019.

Neuenschwander, A., Pitts, K., Jelley, B., Robbins, J., Markel, J., Popescu, S., Nelson, R., Harding, D., Pederson, D., Klotz, B., et al.: Ice, Cloud, and Land Elevation Satellite 2 (ICESat-2) algorithm

theoretical basis document (ATBD) for land-vegetation along-track products (ATL08), National Aeronautics and Space Administration: Washington, DC, USA, 2019.

Smith, B., Fricker, H., Gardner, A., Siegfried, M., Adusumilli, S., Csathó, B., Holschuh, N., Nilsson, J., and Paolo, F.: The ICESat-2 Science Team: ATLAS/ICESat-2 L3A Land Ice Height, Version 2, subset: ATL06_ATLAS/ICESat-2 L3A Glacier Elevation/Ice Sheet Elevation (HDF5), NSIDC: National Snow and Ice Data Center, Boulder, Colorado, USA, 2019a.

Smith, B., Fricker, H. A., Holschuh, N., Gardner, A. S., Adusumilli, S., Brunt, K. M., Csatho, B., Harbeck, K., Huth, A., Neumann, T., et al.: Land ice height-retrieval algorithm for NASA's ICESat-2 photon-counting laser altimeter, Remote Sensing of Environment, 233, 111 352, 2019b.

Smith, B., Hancock, D., Harbeck, K., Roberts, L., Neumann, T., Brunt, K., Fricker, H., Gardner, A., Siegfried, M., Adusumilli, S., et al.: ICE CLOUD and Land Elevation Satellite-2 (ICESat-2) Project Algorithm Theoretical Basis Document (ATBD) For Land Ice Along-Track Height Product (ATL06), NASA Goddard Space Flight Center, Greenbelt, MD, 2021.